

FastFlowNet: A Lightweight Network for Fast Optical Flow Estimation

Lingtong Kong[♣], Chunhua Shen[♣], Jie Yang^{♣,†}

Abstract—Dense optical flow estimation plays a key role in many robotic vision tasks. It has been predicted with satisfying accuracy than traditional methods with advent of deep learning. However, current networks often occupy large number of parameters and require heavy computation costs. These drawbacks have hindered applications on power- or memory-constrained mobile devices. To deal with these challenges, in this paper, we dive into designing efficient structure for fast and accurate optical flow prediction. Our proposed FastFlowNet works in the well-known coarse-to-fine manner with following innovations. First, a new head enhanced pooling pyramid (HEPP) feature extractor is employed to intensify high-resolution pyramid feature while reducing parameters. Second, we introduce a novel center dense dilated correlation (CDDC) layer for constructing compact cost volume that can keep large search radius with reduced computation burden. Third, an efficient shuffle block decoder (SBD) is implanted into each pyramid level to accelerate flow estimation with marginal drops in accuracy. Experiments on both synthetic Sintel and real-world KITTI datasets demonstrate the effectiveness of proposed approaches, which consumes only 1/10 computation of comparable networks to get 90% of their performance. In particular, FastFlowNet only contains 1.37 M parameters and runs at 90 or 5.7 fps with one desktop NVIDIA GTX 1080 Ti or embedded Jetson TX2 GPU on Sintel resolution images.

I. INTRODUCTION

Optical flow estimation is fundamental in a variety of computer vision tasks, including target tracking [1], autonomous navigation [2], obstacle avoidance [3] and action-based human-robot interaction [4][5]. Given time adjacent image frames, optical flow, which represents projected 2D velocity field on image plane, caused by relative 3D motion between an observer and a scene, offers rich information for robotics to interact in complex dynamic environments. With the popularization of smart mobile devices, image sensors and embedded processors have achieved much better performance with a more affordable price, making vision based motion estimation cost effective in robotics. However, extracting meaningful motion information from raw camera data is a complicated and computationally intensive task, where decades of efforts have been made. While traditional methods [6][7][8][9] of optimizing an energy function with brightness constancy and spatial smoothness usually fail in large movement and illuminance change cases, recent deep learning approaches surpass them in both accuracy and running speed thanks to large synthetic datasets and powerful GPUs. Existing Convolutional Neural Networks (CNNs) based architectures can be categorized into two

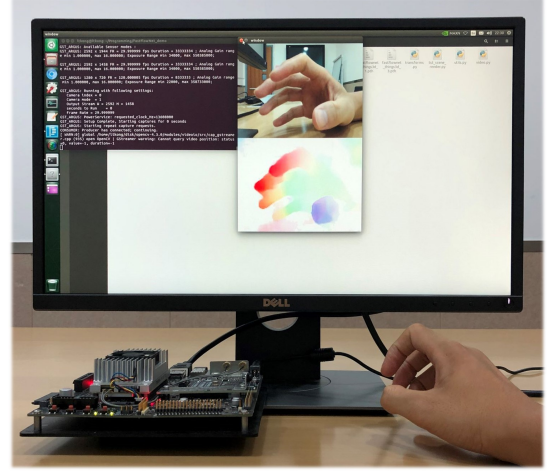


Fig. 1: FastFlowNet can estimate accurate optical flow in real-time on embedded Jetson TX2. Given 384×512 video sequence, it can predict quarter size flow fields at 11 fps.

classes, one is encoder-decoder structure and the other is coarse-to-fine residual structure.

Representative works of the first class are FlowNet [10] and FlowNet2 [11]. The pioneering FlowNet [10] puts up two models named FlowNetS and FlowNetC. They both adopt the U-shape network, specifically, FlowNetS only concatenates two input images while FlowNetC also contains a correlation layer. The successor FlowNet2 [11] further cascade multiple FlowNet models and provide carefully designed learning schedules on multiple datasets. They have shown that CNNs can learn to estimate accurate optical flow with orders of magnitude faster than traditional competitors. However, these networks have to keep large number of channels in low resolutions for feature encoding, resulting in big model size, *e.g.*, FlowNet2 contains more than 160M parameters. Moreover, the correlation layer in FlowNetC locates at a relative high resolution with large search radius, which leads to heavy computation burden. Both defects have hindered them for lightweight mobile applications.

On the other hand, some approaches try to estimate residual flow among decomposed spatial levels where SPyNet [12] is the beginning. It first constructs image pyramids, then concatenates upsampled prior flow, first image and warped second image to estimate residual flow fields in a coarse-to-fine manner. Since each sub module is only responsible for the small magnitude residual flow, SPyNet [12] can approach accuracy of FlowNet [10] with only 1.2M parameters. The main shortcomings are obvious

[♣] Institute of Image Processing and Pattern Recognition, Shanghai Jiao Tong University, China. [♣] The University of Adelaide, Australia.

[†] Corresponding author.

Code is available at <https://github.com/ltkong218/FastFlowNet>

performance degradation and large computation cost at high resolutions. Almost at the same time, PWC-Net [13] and LiteFlowNet [14] replace image pyramid with better feature pyramid and introduce correlation layer into each spatial level for better correspondence representation. Highly ranked results confirm the effectiveness of coarse-to-fine based approaches, where great attention has been paid in following works [15][16][17][18][19][20]. Nevertheless, most recent researches [17][19][21] have focused almost exclusively on pursuing accuracy, the resulting computation intensive algorithms are hardly deployed on energy-constrained embedded devices, such as unmanned aerial vehicles (UAV) and micro intelligent robots. Also, their large number of parameters will occupy lots of storage space and increase the risk of overfitting. In fact, we will show that the efficient LiteFlowNet [14] barely breaks the 1 FPS barrier when inferring Sintel resolution images (436×1024) on Jetson TX2, which is far from practical deployment.

To speed up accurate optical flow estimation and facilitate practical applications, we propose a lightweight and fast network dubbed FastFlowNet in this paper. Our model is based on widely used coarse-to-fine residual structure and we improve it on three aspects, that is pyramid feature extraction, cost volume construction and optical flow decoding, covering all components of flow estimation pipeline. First, we present a head enhanced pooling pyramid (HEPP) feature extractor, which uses convolution layer in higher levels while adopting parameter free pooling in other lower levels. This efficient module can be regarded as combination of feature pyramid in PWC-Net [13] and pooling pyramid of SPyNet [12], that aims to extract relative good matching feature with obviously reduced parameters and computation. Second, recent studies [13] [19] have shown that increasing search radius of correlation layer can improve flow accuracy, however, feature channels of cost volume are square to search radius and computation complexity of following decoder network will be fourth power of search radius. In FastFlowNet, we keep search radius to 4 as PWC-Net [13] for perceiving large movement. Differently, to reduce computation burden, we down sample feature channels in large residual regions and propose a novel center dense dilated correlation (CDDC) layer for constructing compact cost volume. Our motivation is that residual flow distributions are more focused on small motion, and experiments show that CDDC behaves better than other compression methods. Third, we observe that flow decoders in each pyramid level occupy a relatively large proportion of parameters and computation as for the whole network. To further reduce computation and meanwhile hold superior performance, we build a new shuffle block decoder (SBD) module referring to the lightweight ShuffleNet [22], for its low computation budget and high classification precision. Different from ShuffleNet [22] as a backbone network, our SBD module is employed for regressing optical flow, that is only located in the middle part of decoder network. The overall architecture of FastFlowNet is depicted in Fig 2.

Based on above improvements, proposed network can achieve advanced performance on Sintel [23] and KITTI [24]

benchmarks with significantly reduced computation budget. In particular, FastFlowNet runs $3\times$ faster than PWC-Net [13] with $1/7$ computation and $5\times$ faster than LiteFlowNet [14] with $1/13$ computation when predicting quarter resolution flow fields. Moreover, it only contains 1.37 M parameters which is as light as SPyNet [12], but behaves much better with $5\times$ speed up, confirming state-of-the-art size-accuracy trade-off. Thanks to the coarse-to-fine structure, FastFlowNet can naturally trade accuracy for speed according to specific robotic applications. For example, our model can process 436×1024 resolution images within a range of 5.7-26 fps on one Jetson TX2 GPU. To our best knowledge, FastFlowNet represents the first real-time solution for accurate optical flow on embedded devices as shown in Fig 1.

II. RELATED WORK

FlowNet [10] is the first work to use CNNs for optical flow estimation. It propose two variants of FlowNetS and FlowNetC together with the synthetic FlyingChairs dataset for end-to-end training. The successor FlowNet2 [11] fuses cascaded FlowNets with a small displacement module, and use FlyingThings3D [25] dataset for a further fine-tuning schedule. These encoder-decoder based networks have exceeded variational solutions with orders of magnitude faster speed, however, large model sizes make them unfit for lightweight mobile applications.

Inspired by traditional image pyramid, SPyNet [12] estimates residual flow in decomposed spatial levels with only 1.2M parameters, whereas, it suffers from performance degradation. Following coarse-to-fine residual structures, *i.e.*, PWC-Net [13] and LiteFlowNet [14] employ feature pyramid, warping and correlation in each level to succeed in raising accuracy with reduced parameters, representing the most efficient optical flow architecture. Following researches are almost exclusively focused on improving accuracy. IRR-PWC [15] shares flow decoder and context network among all spatial scales for joint optical flow and occlusion estimation. HD3-Flow [16] decomposes contiguous flow fields into discrete grids and adopts a better backbone. FD-FlowNet [18] employs better U-shape network and partial fully connected flow estimators for efficient inference. MaskFlowNet [17] adds additional occlusion mask module into PWC-Net [13] with cascaded refinement. Recently, RAFT [21] outperforms other approaches by first calculating all-pairs similarity and then performing a dozen iterations at high resolution, however, it incurs huge computation burden. In short, we should highlight that the efficient LiteFlowNet [14] only runs at 1.1 fps when inferring Sintel resolution images on Jetson TX2 GPU, which is not suitable for low-power devices, let alone other heavy models.

III. FASTFLOWNET

A. Approach Overview

Given two time-adjacent input images $I_1, I_2 \in \mathbb{R}^{H \times W \times 3}$, proposed FastFlowNet exploits the coarse-to-fine residual structure to estimate gradually refined optical flow $F^l \in \mathbb{R}^{H^l \times W^l \times 2}, l = 6, 5, \dots, 2$, but it is extensively reformed

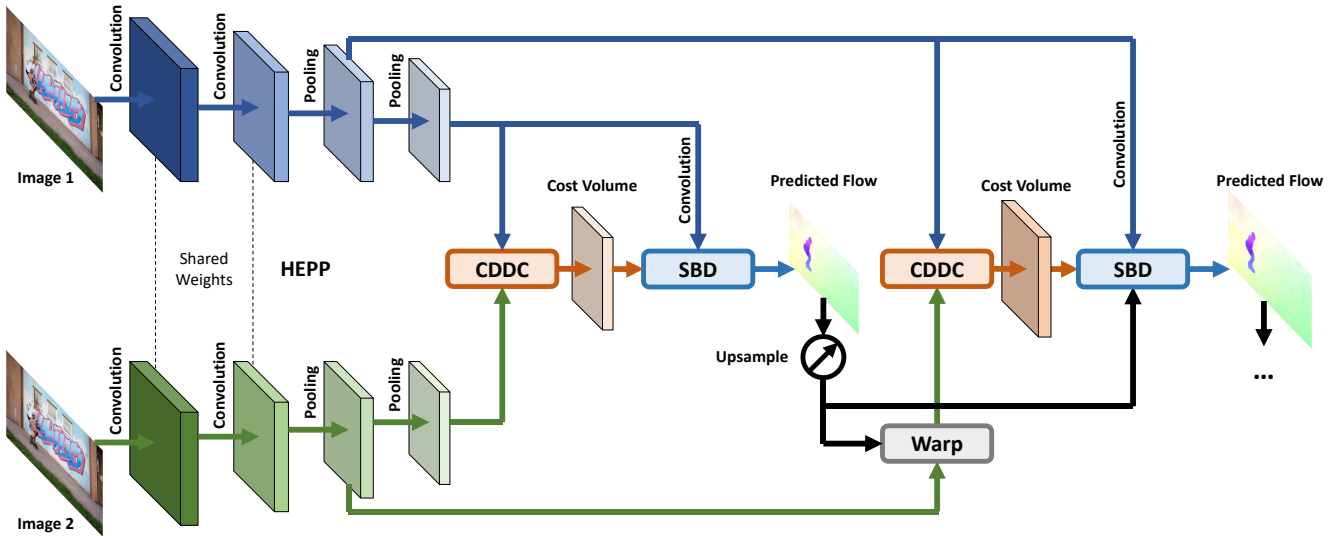


Fig. 2: Architecture overview of FastFlowNet. HEPP, CDDC and SBD are efficient modules for extracting pyramid feature, constructing cost volume and regressing optical flow respectively. Only two levels are shown for clarity.

to accelerate inference by properly reducing parameters and computation cost. To this end, we first change the dual convolution feature pyramid in PWC-Net [13] to head enhanced pooling pyramid for enhancing high resolution pyramid feature and reducing model size. Then we propose a novel center dense dilated correlation layer for constructing compact cost volume while keeping large search radius. Finally, new shuffle block decoders are employed in each pyramid level to regress optical flow with obvious reduction on computation and marginal drops in accuracy. The overall architecture of FastFlowNet is depicted in Fig 2, and structure details are listed in Table I.

B. Head Enhanced Pooling Pyramid

Traditional methods [26][7] apply image pyramid into optical flow estimation for speeding up optimization or dealing with large displacement. SPyNet [12] succeeds to transfer classical paradigm and first introduces pooling based image pyramid into deep models. Since raw images are variant to illuminance changes and the fixed pooling pyramid is vulnerable to noise [27], such as shadows and reflection, PWC-Net [13] and LiteFlowNet [14] replace it by learnable feature pyramid with significant improvement. Concretely, they gradually expands feature channels while shrinking spatial size by half to extract robust matching feature.

However, large channel numbers in low resolutions will occupy lots of parameters. Moreover, it can be redundant for coarse-to-fine structure, since low level pyramid features are only responsible to estimate coarse flow fields. Thus, we combine feature pyramid in high levels with pooling pyramid in other low levels to obtain both strengths as shown in Fig 2. On the other hand, high resolution pyramid feature is relatively shallow in PWC-Net, as each pyramid level only contains two convolutions with 3×3 kernel that has small receptive field. So we add one more convolution in high

levels to intensify pyramid feature with small extra cost. By balancing computation among different scales, we have presented a head enhanced pooling pyramid feature extractor as listed in the top of Table I. Like FlowNetC, PWC-Net and LiteFlowNet, HEPP generates six pyramid levels from $1/2$ resolution (level 1) to $1/64$ resolution (level 6) by a scale factor of 2.

C. Center Dense Dilated Correlation

One crucial step in modern optical flow architectures is to calculate feature correspondence by the inner product based correlation layer [10]. Given two pyramid features of f_1^l, f_2^l in level l , like many coarse-to-fine residual approaches, we first adopt the bilinear interpolation based warping operation [12][11] to warp the second feature f_2^l according to $2 \times$ upsampled previous flow field $up_2(F^{l+1})$. The warped target feature f_{warp}^l can significantly reduce displacement caused by large motion, that helps to narrow search region and simplify the task to estimate relatively small residual flow. Recent models [13][14] construct cost volume by correlating source feature with corresponding warped target features within a local square area that can be formulated as

$$c^l(\mathbf{x}, \mathbf{d}) = f_1^l(\mathbf{x}) \cdot f_{warp}^l(\mathbf{x} + \mathbf{d}) / N, \mathbf{d} \in [-r, r] \times [-r, r] \quad (1)$$

where \mathbf{x} and \mathbf{d} represent spatial and offset coordinates. N is the length of input features. r means search radius. And \cdot stands for inner product.

Existing works [13][19] have shown that increasing search radius when building cost volume can lead to lower end point error during both training and testing, especially for large displacement cases. However, feature channels of cost volume are square to search radius and computation complexity of following decoder network will be fourth power. As shown in Fig 3a, many flow networks [13][18][15][16] set $r = 4$, and the resulting large computation burden has impeded low-power applications. An easy way to reduce computation cost

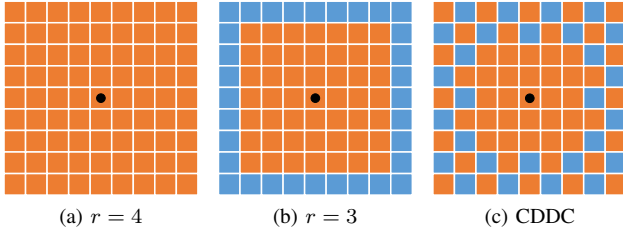


Fig. 3: Different approaches for constructing cost volume. Orange squares represent considered search grids. (a) and (b) are traditional square matching costs while (c) is the new proposed center dense dilated cost volume.

is to decrease r , such as setting $r = 3$ in Fig 3b. It can reduce cost volume features from 81 to 49, however this method is at the expense of sacrificing perception range and accuracy.

Inspired by the atrous spatial pyramid pooling (ASPP) module in DeepLabv3 [28], we propose a novel center dense dilated correlation (CDDC) layer that samples search grids densely around the center while down sampling grid points in large motion areas as shown in Fig 3c. Different from ASPP which uses parallel atrous convolutions to capture multi-scale context information, proposed CDDC is designed to reduce computation when constructing large radius cost volume. In FastFlowNet, it outputs 53 feature channels which has similar computation budget with traditional $r = 3$ setting. Our motivation is that residual flow distribution is more focused on small motions, and experiments will show that CDDC behaves better than naive compression method.

D. Shuffle Block Decoder

After building cost volume, coarse-to-fine models usually concatenate context feature, cost volume and upsampled previous flow as inputs for following decoder networks. Existing in each pyramid level, the decoder part takes up most parameters and computation of the whole network. Thus, better speed-accuracy trade-off is worth investigation.

PWC-Net [13] shows that dense connected flow decoder can improve accuracy after fine-tuning on FlyingThings3D [25] dataset at the price of increasing model size and computation. LiteFlowNet [14] uses sequential connected flow estimator and also gets relative good performance. To achieve better trade-off between these two topologies, FDFlowNet [18] employs partial fully connected structure. However, all these methods can not well support real-time inference on embedded systems.

Thanks to compact cost volume built by CDDC, we can directly decrease maximal feature channel in decoder network from previous 128 to current 96 without convergence issue. To further reduce computation and model size, we reform the middle three 96 channel convolutions into group convolution followed by channel shuffle operations, which we call it shuffle block. Different from ShuffleNet [22] as a backbone network, our shuffle block decoder is employed for regressing optical flow. As listed in the bottom of Table I, each decoder network contains three shuffle blocks with

TABLE I: Architecture of FastFlowNet. HEPP, MFC, SBD represents head enhanced pooling pyramid, multiple feature construction and shuffle block decoder. MFC and SBD share the same structure across all pyramid levels, thus only level 5 are listed for brevity. Pool stands for average pooling. Fconv5_2, fconv5_3 and fconv5_4 are convolutions with group=3. Shuffle means channel shuffle operation [22]. Convolution layers except upconv6 (deconvolution) and fconv5_7 are followed by LeakyReLU activation.

	Layer Name	Kernel	Stride	Input	Ch I/O
HEPP	pconv1.1	3×3	2	img1 or img2	3/16
	pconv1.2	3×3	1	pconv1.1	16/16
	pconv2.1	3×3	2	pconv1.2	16/32
	pconv2.2	3×3	1	pconv2.1	32/32
	pconv2.3	3×3	1	pconv2.2	32/32
	pconv3.1	3×3	2	pconv2.3	32/64
	pconv3.2	3×3	1	pconv3.1	64/64
	pconv3.3	3×3	1	pconv3.2	64/64
	pool4	2×2	2	pconv3.3	64/64
	pool5	2×2	2	pool4	64/64
	pool6	2×2	2	pool5	64/64
MFC	upconv6	4×4	1/2	flow6	2/2
	warp5	-	-	pool5b, upconv6	64, 2/64
	cdcc5	1×1	1	pool5a, warp5	64, 64/53
	rconv5	3×3	1	pool5a	64/32
	concat5	rconv5 + cdcc5 + upconv6			32, 53, 2/87
SBD	fconv5.1	3×3	1	concat5	87/96
	fconv5.2	3×3	1	fconv5.1	3×32/3×32
	shuffle5.2	-	-	fconv5.2	3×32/32×3
	fconv5.3	3×3	1	shuffle5.2	3×32/3×32
	shuffle5.3	-	-	fconv5.3	3×32/32×3
	fconv5.4	3×3	1	shuffle5.3	3×32/3×32
	shuffle5.4	-	-	fconv5.4	3×32/32×3
	fconv5.5	3×3	1	shuffle5.4	96/64
	fconv5.6	3×3	1	fconv5.5	64/32
	fconv5.7	3×3	1	fconv5.6	32/2

group = 3, that can efficiently reduce computation with marginal drops in accuracy.

E. Loss Function

Since FastFlowNet has the same pyramid scales as FlowNet [10] and PWC-Net [13], we adopt the same multi-scale L2 loss for training

$$L_{epe} = \sum_{l=2}^6 \alpha_l \sum_{\mathbf{x}} |F^l(\mathbf{x}) - F_{gt}^l(\mathbf{x})|_2 \quad (2)$$

where $|\cdot|_2$ computes L2 norm between predicted and ground-truth flow fields. When fine-tuning on datasets with real scene structure, such as KITTI, we use following robust loss

$$L_{robust} = \sum_{l=2}^6 \alpha_l \sum_{\mathbf{x}} (|F^l(\mathbf{x}) - F_{gt}^l(\mathbf{x})| + \epsilon)^q \quad (3)$$

where $|\cdot|$ denotes L1 norm, $\epsilon = 0.01$ is a small constant and $q < 1$ makes loss more robust for large magnitude outliers. For fair comparison with previous methods [10][11][13][14], weights in Eq 2 and Eq 3 are set to $\alpha_6 = 0.32, \alpha_5 = 0.08, \alpha_4 = 0.02, \alpha_3 = 0.01$ and $\alpha_2 = 0.005$.

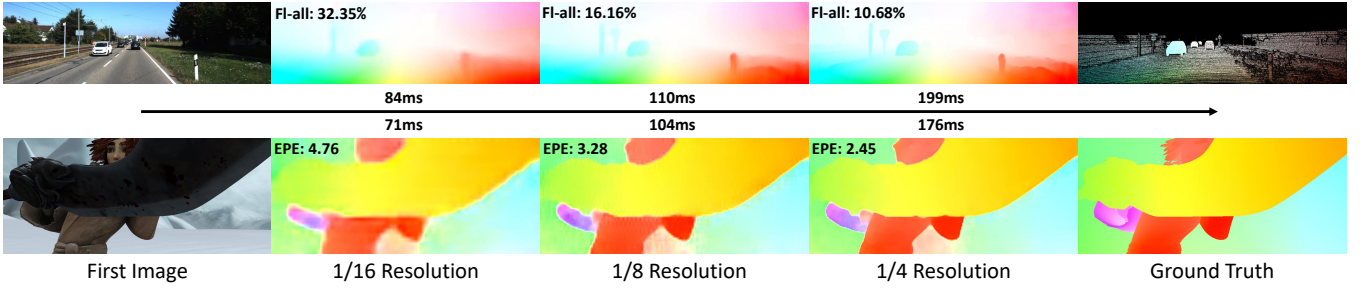


Fig. 4: Visual examples of anytime inference. FastFlowNet can naturally trade speed for accuracy according to specific robotic applications. Black arrow means inference timeline which is measured on embedded Jetson TX2 GPU.

TABLE II: Ablation study on structure variants with different pyramid feature extractor, cost volume constructor and optical flow decoder. Flow accuracy is measured by end point error. FLOPs are calculated on Sintel resolution images.

Pyramid	Cost	Decoder	Sintel	KITTI	Params	FLOPs
conv	$r = 4$	$g = 1$	3.12	2.37	4.23M	28.2G
conv+pool	$r = 4$	$g = 1$	3.00	2.25	3.22M	27.7G
HEPP	$r = 4$	$g = 1$	2.92	2.13	3.27M	28.3G
HEPP	$r = 3$	$g = 1$	2.93	2.33	2.18M	19.1G
HEPP	CDDC	$g = 1$	2.95	2.18	2.20M	19.2G
HEPP	CDDC	$g = 2$	3.04	2.22	1.57M	14.0G
HEPP	CDDC	$g = 3$	3.11	2.29	1.37M	12.2G
HEPP	CDDC	$g = 4$	3.22	2.47	1.26M	11.3G
HEPP	CDDC	$g = 6$	3.35	2.59	1.16M	10.4G

IV. EXPERIMENTS

A. Implementation Details

To compare FastFlowNet with other networks, we follow the two-stage training strategy proposed in FlowNet2 [11]. Ground truth optical flow is divided by 20 and down sampled as supervision at different levels. Since final flow prediction is in quarter resolution, we use bilinear interpolation to obtain the full resolution optical flow. During both training and fine-tuning, we use the same data augmentation methods as [11], including mirror, translate, rotate, zoom, squeeze and color jitter. All our experiments are implemented in PyTorch and conducted on a machine equipped with 4 NVIDIA GTX 1080 Ti GPU cards. To compare performance of different optical flow models on mobile device, we further evaluate inference delay on the embedded Jetson TX2 GPU.

We first train FastFlowNet on FlyingChairs [10] using S_{short} learning schedule [11], *i.e.*, learning rate is initially set to $1e-4$ and decays half at 300k, 400k and 500k iterations. We crop 320×448 patches during data augmentation and adopt a batch size of 8. Then the model is fine-tuned on FlyingThings3D [25] using the S_{fine} schedule [11], *i.e.*, learning rate is initially set to $1e-5$ and decays half at 200k, 300k and 400k iterations. Random crop size is 384×768 and batch size is set to 4. Adam [29] optimizer and multi-scale L2 loss in Eq 2 are always used. We call the model **FastFlowNet** after above two-stage learning schedules whose results on Sintel and KITTI training sets are listed in Table III.

B. Ablation Study

To explore efficient optical flow structure with low computation cost, we do ablations on pyramid feature extractor, cost volume constructor and optical flow decoder. Results of the gradually lightened models are as listed in Table II. All variants are first trained on FlyingChairs and evaluated on Sintel Clean training sets. To test in large displacement cases, that are common when robots move forward or backward, then they are fine-tuned on KITTI 2015 training subset for 5-fold cross-validation. Since change of inference delay is not distinct based on PyTorch implementation, we use FLOPs [30][22] which means number of floating point multiply-add operations to measure real computation complexity. In Table II, 'conv' represents dual convolution feature pyramid used in PWC-Net, 'conv+pool' stands for combining dual convolution feature pyramid in top 3 levels with pooling pyramid in bottom 3 levels. Note that traditional $r = 4$ cost volume has sequential connected flow decoders, whose maximal feature channel is 128 rather than 96, in order to make it fully convergent. $g = 1$ means no grouping convolution without shuffle block in flow decoder.

Surprisingly, the lighter 'conv+pool' pyramid feature extractor behaves better than traditional 'conv' method. Our analysis is that parameter free average pooling can share gradients among different levels during backpropagation that makes pyramid feature more robust to scale change. By replacing 'conv+pool' with HEPP, we can get better results with small additional overhead. Then, we decrease search radius for constructing lightened $r = 3$ cost volume to reduce energy consumption. Flow accuracy on Sintel has almost no change, while results on large displacement KITTI decline obviously. To mitigate performance degradation, we adopt CDDC to build compact cost volume with larger receptive field in each pyramid level. Though it does not improve on Sintel training which contains lots of small movements, it behaves better on more challenging KITTI 2015 validation set. Finally, we employ SBD for further compression on parameters and computation. In Table III, we gradually lighten the network by setting incremental group numbers in SBD. It can be seen that computation reduction becomes relatively small when $g > 3$, whereas obvious performance degradation appears. Thus, we adopt $g = 3$ in FastFlowNet which gets better computation-accuracy trade-off.

TABLE III: Performance comparison on benchmarks. Speed and computation are measured on Sintel resolution images. Values in parentheses are results of networks on the data they were trained on. Default accuracy metric is end point error.

Method	Sintel Clean		Sintel Final		KITTI 2012		KITTI 2015			Params (M)	FLOPs (G)	Time (s)	
	train	test	train	test	train	test	train	train(FI-all)	test(FI-all)			1080Ti	TX2
FlowNetC [10]	4.31	7.28	5.87	8.81	9.35	-	-	-	-	39.18	6055.3	0.029	0.427
FlowNetC-ft	(3.78)	6.85	(5.28)	8.51	8.79	-	-	-	-	39.18	6055.3	0.029	0.427
FlowNet2 [11]	2.02	3.96	3.14	6.02	4.09	-	10.06	30.37%	-	162.52	24836.4	0.116	1.547
FlowNet2-ft	(1.45)	4.16	(2.01)	5.74	(1.28)	1.8	(2.30)	(8.61%)	11.48%	162.52	24836.4	0.116	1.547
SPyNet [12]	4.12	6.69	5.57	8.43	9.12	-	-	-	-	1.20	149.8	0.050	0.918
SPyNet-ft	(3.17)	6.64	(4.32)	8.36	(4.13)	4.7	-	-	35.07%	1.20	149.8	0.050	0.918
PWC-Net [13]	2.55	-	3.93	-	4.14	-	10.35	33.67%	-	8.75	90.8	0.034	0.485
PWC-Net-ft	(2.02)	4.39	(2.08)	5.04	(1.45)	1.7	(2.16)	(9.80%)	9.60%	8.75	90.8	0.034	0.485
LiteFlowNet[14]	2.48	-	4.04	-	4.00	-	10.39	28.50%	-	5.37	163.5	0.055	0.907
LiteFlowNet-ft	(1.35)	4.54	(1.78)	5.38	(1.05)	1.6	(1.62)	(5.58%)	9.38%	5.37	163.5	0.055	0.907
PWC-Net-small	2.83	-	4.08	-	-	-	-	-	-	4.08	-	0.024	-
LiteFlowNetX	3.58	-	4.79	-	6.38	-	15.81	34.90%	-	0.90	-	0.035	-
FastFlowNet	2.89	-	4.14	-	4.84	-	12.24	33.10%	-	1.37	12.2	0.011	0.176
FastFlowNet-ft	(2.08)	4.89	(2.71)	6.08	(1.31)	1.8	(2.13)	(8.21%)	11.22%	1.37	12.2	0.011	0.176

C. MPI Sintel

When fine-tuning on Sintel [23] training sets, we crop 320×768 patches and set batch size to 4. Robust loss in Eq 3 is adopted with $q = 0.4$. Like PWC-Net, we set initial learning rate to $5e - 5$ and disturb it to $3e - 5$, $2e - 5$ and $1e - 5$ every 150k iterations in total 600k iterations to jump out from local minimum, where learning rate decays to zero in each period. We report results on Sintel test sets by submitting predictions on MPI Sintel online benchmark, which are listed in Table III. For mobile applications, we also measure computation burden of different networks in FLOPs and real inference delay on both desktop GTX 1080Ti GPU and embedded Jetson TX2. All experiments are conducted in PyTorch for fair comparison.

In Table III, FastFlowNet outperforms FlowNetC [10] in all items due to the advanced coarse-to-fine residual structure. It runs $2.5 \times$ faster than FlowNetC on both GTX 1080Ti and Jetson TX2 with $500 \times$ less computation. The reason why computation complexity is not proportional to inference delay is that correlation and warping layers have large memory access cost (MAC) while they are low FLOPs operations. FastFlowNet outperforms SPyNet [12] by 26.4% and 27.3% on Sintel Clean and Final test sets respectively. Though containing a little more parameters, our network runs $5 \times$ faster with $12 \times$ less computation. Compared with the state-of-the-art LiteFlowNet [14], we can approach 90% of its performance with $13.4 \times$ less (only 12.2 GFLOPs) computation budget. To further verify effectiveness of proposed flow architecture simplification methods, we compare FastFlowNet with small versions of PWC-Net [13] and LiteFlowNet [14] provided in their papers. PWC-Net-small is the small version of PWC-Net by dropping dense connections in flow decoders. And LiteFlowNetX is the small-sized variant by shrinking convolution channels in feature pyramid and flow estimators. We can see that FastFlowNet gets almost the same good results with PWC-Net-small on Sintel training datasets after two-stage pretraining, while being additional $3 \times$ smaller and $2 \times$ faster.

D. KITTI

To test proposed architecture on more challenging large displacement real world data, we fine-tune FastFlowNet on mixed KITTI 2012 [31] and KITTI 2015 [24] training sets. Like [11][13][14], we crop 320×896 patches and adopt batch size 4. The same fine-tuning schedule on Sintel is employed and q in robust loss is set to 0.2 for outlier suppression. To adapt to driving scenes, spatial augmentation methods of rotate, zoom and squeeze are skipped with a probability of 0.5 as [13][14]. Then we evaluate fine-tuned FastFlowNet on the online KITTI benchmarks which are listed in Table III.

Compared with encoder-decoder based FlowNet2 [11], our model can achieve same or better results on KITTI test datasets while being $120 \times$ smaller and $10 \times$ faster. We can get similar accuracy in regard to PWC-Net [13] with $7.5 \times$ less multiply-add computation burden, that is of great concern on low-power embedded systems. For LiteFlowNetX which simply reduces feature channels, proposed HEPP, CDDC and SBD modules behave better on all metrics confirming effectiveness of our contribution. Some visual results in anytime setting [32][33] are depicted in Fig 4.

V. CONCLUSIONS

In this paper, we have proposed a fast and lightweight network for accurate optical flow estimation towards mobile applications. It is based on the well-known coarse-to-fine structure and is extensively reformed to accelerate inference by properly reducing parameters and computation. The proposed head enhanced pooling pyramid, center dense dilated correlation and shuffle block decoder are efficient modules for pyramid feature extraction, cost volume construction and optical flow decoding, that covers all components of flow estimation pipeline. We evaluate them on both synthetic Sintel and real-world KITTI datasets to verify their effectiveness. The proposed FastFlowNet can be directly plugged into any optical flow based robotic vision systems with much less resource consumption and nice performance.

REFERENCES

- [1] K. Shuang, Y. Huang, Y. Sun, Z. Cai, and H. Guo, "Fine-grained motion representation for template-free visual tracking," in *2020 IEEE Winter Conference on Applications of Computer Vision (WACV)*, 2020, pp. 660–669.
- [2] C. Wang, T. Ji, T. Nguyen, and L. Xie, "Correlation flow: Robust optical flow using kernel cross-correlators," in *2018 IEEE International Conference on Robotics and Automation (ICRA)*, 2018, pp. 836–841.
- [3] Kahlouche Souhila and Achour Karim, "Optical flow based robot obstacle avoidance," *International Journal of Advanced Robotic Systems*, vol. 4, no. 1, pp. 2, 2007.
- [4] J. Chang, A. Tejero-de-Pablos, and T. Harada, "Improved optical flow for gesture-based human-robot interaction," in *2019 International Conference on Robotics and Automation (ICRA)*, 2019, pp. 7983–7989.
- [5] Xiaohang Yang, Lingtong Kong, and Jie Yang, "Unsupervised motion representation enhanced network for action recognition," in *2021 IEEE International Conference on Acoustics, Speech and Signal Processing (ICASSP)*, 2021.
- [6] Berthold K. P. Horn and Brian G. Schunck, "Determining optical flow," in *Artif. Intell.*, 1981.
- [7] Thomas Brox and Jitendra Malik, "Large displacement optical flow: Descriptor matching in variational motion estimation," in *IEEE transactions on pattern analysis and machine intelligence*, 2011.
- [8] C. Zach, T. Pock, and H. Bischof, "A duality based approach for realtime tv-l1 optical flow," in *Pattern Recognition*, Fred A. Hamprecht, Christoph Schnörr, and Bernd Jähne, Eds., 2007.
- [9] Till Kroeger, Radu Timofte, Dengxin Dai, and Luc Van Gool, "Fast optical flow using dense inverse search," in *Computer Vision – ECCV 2016*, Bastian Leibe, Jiri Matas, Nicu Sebe, and Max Welling, Eds., 2016.
- [10] Philipp Fischer, Alexey Dosovitskiy, Eddy Ilg, Philip Häusser, Caner Hazirbas, Vladimir Golkov, Patrick van der Smagt, Daniel Cremers, and Thomas Brox, "FlowNet: Learning optical flow with convolutional networks," in *2015 IEEE International Conference on Computer Vision (ICCV)*, 2015.
- [11] Eddy Ilg, Nikolaus Mayer, Tonmoy Saikia, Margret Keuper, Alexey Dosovitskiy, and Thomas Brox, "FlowNet 2.0: Evolution of optical flow estimation with deep networks," in *2017 IEEE Conference on Computer Vision and Pattern Recognition (CVPR)*, 2017.
- [12] Anurag Ranjan and Michael J. Black, "Optical flow estimation using a spatial pyramid network," in *2017 IEEE Conference on Computer Vision and Pattern Recognition (CVPR)*, 2017.
- [13] Deqing Sun, Xiaodong Yang, Ming-Yu Liu, and Jan Kautz, "Pwc-net: Cnns for optical flow using pyramid, warping, and cost volume," in *The IEEE Conference on Computer Vision and Pattern Recognition (CVPR)*, 2018.
- [14] Tak-Wai Hui, Xiaoou Tang, and Chen Change Loy, "LiteflowNet: A lightweight convolutional neural network for optical flow estimation," in *The IEEE Conference on Computer Vision and Pattern Recognition (CVPR)*, 2018.
- [15] Junhwa Hur and Stefan Roth, "Iterative residual refinement for joint optical flow and occlusion estimation," in *The IEEE Conference on Computer Vision and Pattern Recognition (CVPR)*, 2019.
- [16] Zhichao Yin, Trevor Darrell, and Fisher Yu, "Hierarchical discrete distribution decomposition for match density estimation," in *The IEEE Conference on Computer Vision and Pattern Recognition (CVPR)*, June 2019.
- [17] Shengyu Zhao, Yilun Sheng, Yue Dong, Eric I-Chao Chang, and Yan Xu, "MaskflowNet: Asymmetric feature matching with learnable occlusion mask," in *Proceedings of the IEEE Conference on Computer Vision and Pattern Recognition (CVPR)*, 2020.
- [18] Lingtong Kong and Jie Yang, "FdfloNet: Fast optical flow estimation using a deep lightweight network," in *2020 IEEE International Conference on Image Processing (ICIP)*, 2020.
- [19] Markus Hofinger, Samuel Rota Bulò, Lorenzo Porzi, Arno Knapitsch, Thomas Pock, and Peter Kontschieder, "Improving optical flow on a pyramid level," in *European Conf. on Computer Vision (ECCV)*, 2020.
- [20] Lingtong Kong, Xiaohang Yang, and Jie Yang, "Oas-net: Occlusion aware sampling network for accurate optical flow," in *2021 IEEE International Conference on Acoustics, Speech and Signal Processing (ICASSP)*, 2021.
- [21] Zachary Teed and Jia Deng, "RAFT: Recurrent all-pairs field transforms for optical flow," in *European Conf. on Computer Vision (ECCV)*, 2020.
- [22] X. Zhang, X. Zhou, M. Lin, and J. Sun, "ShuffleNet: An extremely efficient convolutional neural network for mobile devices," in *2018 IEEE/CVF Conference on Computer Vision and Pattern Recognition*, 2018.
- [23] D. J. Butler, J. Wulff, G. B. Stanley, and M. J. Black, "A naturalistic open source movie for optical flow evaluation," in *European Conf. on Computer Vision (ECCV)*, 2012.
- [24] M. Menze and A. Geiger, "Object scene flow for autonomous vehicles," in *2015 IEEE Conference on Computer Vision and Pattern Recognition (CVPR)*, 2015, pp. 3061–3070.
- [25] N. Mayer, E. Ilg, P. Häusser, P. Fischer, D. Cremers, A. Dosovitskiy, and T. Brox, "A large dataset to train convolutional networks for disparity, optical flow, and scene flow estimation," in *IEEE International Conference on Computer Vision and Pattern Recognition (CVPR)*, 2016.
- [26] Jean yves Bouguet, "Pyramidal implementation of the lucas kanade feature tracker," *Intel Corporation, Microprocessor Research Labs*, 2000.
- [27] Thomas Brox, Andrés Bruhn, Nils Papenberg, and Joachim Weickert, "High accuracy optical flow estimation based on a theory for warping," in *Computer Vision - ECCV 2004*, 2004.
- [28] Liang-Chieh Chen, George Papandreou, Florian Schroff, and Hartwig Adam, "Rethinking atrous convolution for semantic image segmentation," *CoRR*, vol. abs/1706.05587, 2017.
- [29] Diederik P. Kingma and Jimmy Ba, "Adam: A method for stochastic optimization," in *3rd International Conference on Learning Representations, ICLR 2015*, 2015.
- [30] Andrew G. Howard, Menglong Zhu, Bo Chen, Dmitry Kalenichenko, Weijun Wang, Tobias Weyand, Marco Andreetto, and Hartwig Adam, "Mobilenets: Efficient convolutional neural networks for mobile vision applications," *CoRR*, vol. abs/1704.04861, 2017.
- [31] Andreas Geiger, Philip Lenz, and Raquel Urtasun, "Are we ready for autonomous driving? the kitti vision benchmark suite," in *Conference on Computer Vision and Pattern Recognition (CVPR)*, 2012.
- [32] Yan Wang, Zihang Lai, Gao Huang, Brian H. Wang, Laurens Van Der Maaten, Mark Campbell, and Kilian Q Weinberger, "Anytime stereo image depth estimation on mobile devices," in *2019 International Conference on Robotics and Automation (ICRA)*, 2019.
- [33] Pier Luigi Dovesi, Matteo Poggi, Lorenzo Andraghetti, Miquel Martí, Hedvig Kjellström, Alessandro Pieropan, and Stefano Mattoccia, "Real-time semantic stereo matching," in *2020 International Conference on Robotics and Automation (ICRA)*, 2020.